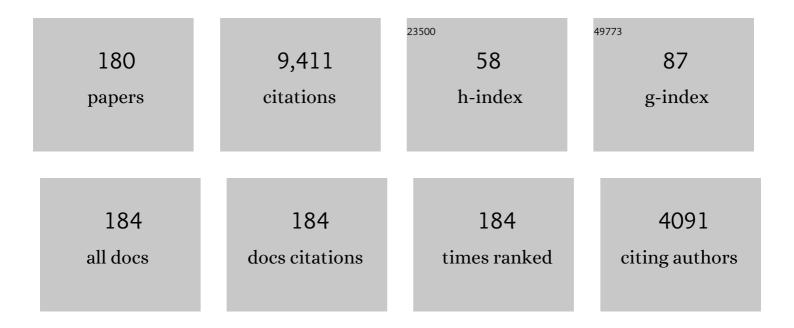
List of Publications by Year in descending order

Source: https://exaly.com/author-pdf/9041204/publications.pdf Version: 2024-02-01



#	Article	IF	CITATIONS
1	A review on high-pressure torsion (HPT) from 1935 to 1988. Materials Science & Engineering A: Structural Materials: Properties, Microstructure and Processing, 2016, 652, 325-352.	2.6	444
2	High-entropy ceramics: Review of principles, production and applications. Materials Science and Engineering Reports, 2021, 146, 100644.	14.8	294
3	High-pressure torsion of pure magnesium: Evolution of mechanical properties, microstructures and hydrogen storage capacity with equivalent strain. Scripta Materialia, 2011, 64, 880-883.	2.6	239
4	Nanomaterials by severe plastic deformation: review of historical developments and recent advances. Materials Research Letters, 2022, 10, 163-256.	4.1	215
5	High-pressure torsion of pure metals: Influence of atomic bond parameters and stacking fault energy on grain size and correlation with hardness. Acta Materialia, 2011, 59, 6831-6836.	3.8	212
6	Microstructure and mechanical properties of pure Cu processed by high-pressure torsion. Materials Science & Engineering A: Structural Materials: Properties, Microstructure and Processing, 2008, 497, 168-173.	2.6	202
7	Influence of dislocation–solute atom interactions and stacking fault energy on grain size of single-phase alloys after severe plastic deformation using high-pressure torsion. Acta Materialia, 2014, 69, 68-77.	3.8	173
8	Significance of homologous temperature in softening behavior and grain size of pure metals processed by high-pressure torsion. Materials Science & Engineering A: Structural Materials: Properties, Microstructure and Processing, 2011, 528, 7514-7523.	2.6	160
9	High-pressure torsion for enhanced atomic diffusion and promoting solid-state reactions in the aluminum–copper system. Acta Materialia, 2013, 61, 3482-3489.	3.8	159
10	Design and synthesis of a magnesium alloy for room temperature hydrogen storage. Acta Materialia, 2018, 149, 88-96.	3.8	157
11	Processing Pure Ti by High-Pressure Torsion in Wide Ranges of Pressures and Strain. Metallurgical and Materials Transactions A: Physical Metallurgy and Materials Science, 2009, 40, 2079-2086.	1.1	149
12	Reversible room temperature hydrogen storage in high-entropy alloy TiZrCrMnFeNi. Scripta Materialia, 2020, 178, 387-390.	2.6	132
13	Hydrogen storage performance of TiFe after processing by ball milling. Acta Materialia, 2015, 88, 190-195.	3.8	131
14	High-pressure torsion of TiFe intermetallics for activation of hydrogen storage at room temperature with heterogeneous nanostructure. International Journal of Hydrogen Energy, 2013, 38, 4622-4627.	3.8	122
15	Significance of grain boundaries and stacking faults on hydrogen storage properties of Mg 2 Ni intermetallics processed by high-pressure torsion. Acta Materialia, 2015, 92, 46-54.	3.8	120
16	Evolution of Mechanical Properties and Microstructures with Equivalent Strain in Pure Fe Processed by High Pressure Torsion. Materials Transactions, 2009, 50, 44-50.	0.4	113
17	Activation of TiFe for hydrogen storage by plastic deformation using groove rolling and high-pressure torsion: Similarities and differences. International Journal of Hydrogen Energy, 2014, 39, 15589-15594.	3.8	113
18	Photocatalytic hydrogen evolution on a high-entropy oxide. Journal of Materials Chemistry A, 2020, 8, 3814-3821.	5.2	111

#	Article	IF	CITATIONS
19	Significance of temperature increase in processing by high-pressure torsion. Materials Science & Engineering A: Structural Materials: Properties, Microstructure and Processing, 2011, 528, 7301-7305.	2.6	108
20	The significance of slippage in processing by high-pressure torsion. Scripta Materialia, 2009, 60, 9-12.	2.6	107
21	Allotropic phase transformation of pure zirconium by high-pressure torsion. Materials Science & Engineering A: Structural Materials: Properties, Microstructure and Processing, 2009, 523, 277-281.	2.6	105
22	High-pressure zinc oxide phase as visible-light-active photocatalyst with narrow band gap. Journal of Materials Chemistry A, 2017, 5, 20298-20303.	5.2	101
23	Room-Temperature Superplasticity in an Ultrafine-Grained Magnesium Alloy. Scientific Reports, 2017, 7, 2662.	1.6	100
24	Plastic deformation and allotropic phase transformations in zirconia ceramics during high-pressure torsion. Scripta Materialia, 2011, 65, 974-977.	2.6	95
25	Influence of severe plastic deformation at cryogenic temperature on grain refinement and softening of pure metals: Investigation using high-pressure torsion. Materials Science & Engineering A: Structural Materials: Properties, Microstructure and Processing, 2014, 613, 103-110.	2.6	95
26	Ultrahigh strength and high plasticity in TiAl intermetallics with bimodal grain structure and nanotwins. Scripta Materialia, 2012, 67, 814-817.	2.6	94
27	Recent advances in metastable alloys for hydrogen storage: a review. Rare Metals, 2022, 41, 1797-1817.	3.6	93
28	Continuous high-pressure torsion. Journal of Materials Science, 2010, 45, 4578-4582.	1.7	90
29	Ultrafine-grained magnesium–lithium alloy processed by high-pressure torsion: Low-temperature superplasticity and potential for hydroforming. Materials Science & Engineering A: Structural Materials: Properties, Microstructure and Processing, 2015, 640, 443-448.	2.6	87
30	Universal Plot for Hardness Variation in Pure Metals Processed by High-Pressure Torsion. Materials Transactions, 2010, 51, 1051-1054.	0.4	86
31	Mechanism of activation of TiFe intermetallics for hydrogen storage by severe plastic deformation using high-pressure torsion. Applied Physics Letters, 2013, 103, .	1.5	83
32	Formation of FeNi with <i>L</i> 1 ₀ -ordered structure using high-pressure torsion. Philosophical Magazine Letters, 2014, 94, 639-646.	0.5	79
33	High-pressure torsion of titanium at cryogenic and room temperatures: Grain size effect on allotropic phase transformations. Acta Materialia, 2014, 68, 207-213.	3.8	78
34	Equal-Channel Angular Pressing and High-Pressure Torsion of Pure Copper: Evolution of Electrical Conductivity and Hardness with Strain. Materials Transactions, 2012, 53, 123-127.	0.4	77
35	Application of high-pressure torsion for consolidation of ceramic powders. Scripta Materialia, 2010, 63, 174-177.	2.6	76
36	Wear resistance and tribological features of pure aluminum and Al–Al2O3 composites consolidated by high-pressure torsion. Wear, 2014, 310, 83-89.	1.5	75

#	Article	IF	CITATIONS
37	High-pressure torsion of aluminum with ultrahigh purity (99.9999%) and occurrence of inverse Hall-Petch relationship. Materials Science & Engineering A: Structural Materials: Properties, Microstructure and Processing, 2017, 679, 428-434.	2.6	75
38	Effect of temperature rise on microstructural evolution during high-pressure torsion. Materials Science & Engineering A: Structural Materials: Properties, Microstructure and Processing, 2018, 714, 167-171.	2.6	74
39	Softening of high purity aluminum and copper processed by high pressure torsion. International Journal of Materials Research, 2009, 100, 1668-1673.	0.1	73
40	Formation of metastable phases in magnesium–titanium system by high-pressure torsion and their hydrogen storage performance. Acta Materialia, 2015, 99, 150-156.	3.8	73
41	Visible-Light-Driven Photocatalytic Hydrogen Generation on Nanosized TiO ₂ -II Stabilized by High-Pressure Torsion. ACS Catalysis, 2016, 6, 5103-5107.	5.5	73
42	New nanostructured phases with reversible hydrogen storage capability in immiscible magnesium–zirconium system produced by high-pressure torsion. Acta Materialia, 2016, 108, 293-303.	3.8	72
43	Ultrahigh hardness and biocompatibility of high-entropy alloy TiAlFeCoNi processed by high-pressure torsion. Materials Science and Engineering C, 2020, 112, 110908.	3.8	72
44	Mechanochemistry of Metal Hydrides: Recent Advances. Materials, 2019, 12, 2778.	1.3	71
45	Age hardening and thermal stability of Al–Cu alloy processed by high-pressure torsion. Materials Science & Engineering A: Structural Materials: Properties, Microstructure and Processing, 2015, 627, 111-118.	2.6	70
46	Transition from poor ductility to room-temperature superplasticity in a nanostructured aluminum alloy. Scientific Reports, 2018, 8, 6740.	1.6	70
47	High-pressure torsion of pure cobalt: hcp-fcc phase transformations and twinning during severe plastic deformation. Applied Physics Letters, 2013, 102, .	1.5	69
48	Hydrogen storage in TiZrNbFeNi high entropy alloys, designed by thermodynamic calculations. International Journal of Hydrogen Energy, 2020, 45, 33759-33770.	3.8	67
49	Developing age-hardenable Al-Zr alloy by ultra-severe plastic deformation: Significance of supersaturation, segregation and precipitation on hardening and electrical conductivity. Acta Materialia, 2021, 203, 116503.	3.8	67
50	Using ring samples to evaluate the processing characteristics in high-pressure torsion. Acta Materialia, 2009, 57, 1147-1153.	3.8	66
51	Phase transformation and nanograin refinement of silicon by processing through high-pressure torsion. Applied Physics Letters, 2012, 101, .	1.5	65
52	In situ production of bulk intermetallic-based nanocomposites and nanostructured intermetallics by high-pressure torsion. Scripta Materialia, 2012, 66, 386-389.	2.6	65
53	Influence of hydrogen on dislocation self-organization in Ni. Acta Materialia, 2017, 135, 96-102.	3.8	65
54	Effect of high-pressure torsion on grain refinement, strength enhancement and uniform ductility of EZ magnesium alloy. Materials Letters, 2018, 212, 323-326.	1.3	65

#	Article	IF	CITATIONS
55	Photocatalytic hydrogen generation on low-bandgap black zirconia (ZrO ₂) produced by high-pressure torsion. Journal of Materials Chemistry A, 2020, 8, 3643-3650.	5.2	65
56	Plastic Deformation of BaTiO ₃ Ceramics by High-pressure Torsion and Changes in Phase Transformations, Optical and Dielectric Properties. Materials Research Letters, 2015, 3, 216-221.	4.1	64
57	Cold Consolidation of Ball-Milled Titanium Powders Using High-Pressure Torsion. Metallurgical and Materials Transactions A: Physical Metallurgy and Materials Science, 2010, 41, 3308-3317.	1.1	62
58	High-pressure torsion of hafnium. Materials Science & Engineering A: Structural Materials: Properties, Microstructure and Processing, 2010, 527, 2136-2141.	2.6	62
59	Ultra-severe plastic deformation: Evolution of microstructure, phase transformation and hardness in immiscible magnesium-based systems. Materials Science & Engineering A: Structural Materials: Properties, Microstructure and Processing, 2017, 701, 158-166.	2.6	62
60	The use of radiography for thickness measurement and corrosion monitoring in pipes. International Journal of Pressure Vessels and Piping, 2006, 83, 736-741.	1.2	61
61	Scaling-Up of High Pressure Torsion Using Ring Shape. Materials Transactions, 2009, 50, 92-95.	0.4	59
62	Metallurgical Alchemy by Ultra-Severe Plastic Deformation via High-Pressure Torsion Process. Materials Transactions, 2019, 60, 1221-1229.	0.4	59
63	High-entropy oxynitride as a low-bandgap and stable photocatalyst for hydrogen production. Journal of Materials Chemistry A, 2021, 9, 15076-15086.	5.2	59
64	Correlations between hardness and atomic bond parameters of pure metals and semi-metals after processing by high-pressure torsion. Scripta Materialia, 2011, 64, 161-164.	2.6	58
65	High-pressure torsion for new hydrogen storage materials. Science and Technology of Advanced Materials, 2018, 19, 185-193.	2.8	57
66	High-Pressure Torsion of Machining Chips and Bulk Discs of Amorphous Zr ₅₀ Cu ₃₀ Al ₁₀ Ni _{10Materials Transactions, 2010, 51, 23-26.}	18>.	56
67	Softening by severe plastic deformation and hardening by annealing of aluminum–zinc alloy: Significance of elemental and spinodal decompositions. Materials Science & Engineering A: Structural Materials: Properties, Microstructure and Processing, 2014, 610, 17-27.	2.6	56
68	Microstructures and Mechanical Properties of Pure V and Mo Processed by High-Pressure Torsion. Materials Transactions, 2010, 51, 1072-1079.	0.4	55
69	Plastic strain and grain size effect on high-pressure phase transformations in nanostructured TiO2 ceramics. Scripta Materialia, 2016, 124, 59-62.	2.6	54
70	Activation of titanium-vanadium alloy for hydrogen storage by introduction of nanograins and edge dislocations using high-pressure torsion. International Journal of Hydrogen Energy, 2016, 41, 8917-8924.	3.8	54
71	Structure and mechanical behavior of ultrafine-grained aluminum-iron alloy stabilized by nanoscaled intermetallic particles. Acta Materialia, 2019, 167, 89-102.	3.8	54
72	Mechanical Synthesis and Hydrogen Storage Characterization of MgVCr and MgVTiCrFe Highâ€Entropy Alloy. Advanced Engineering Materials, 2020, 22, 1901079.	1.6	54

#	Article	IF	CITATIONS
73	Defective high-entropy oxide photocatalyst with high activity for CO2 conversion. Applied Catalysis B: Environmental, 2022, 303, 120896.	10.8	52
74	Review on Recent Advancements in Severe Plastic Deformation of Oxides by Highâ€Pressure Torsion (HPT). Advanced Engineering Materials, 2019, 21, 1800272.	1.6	51
75	Examination of inverse Hall-Petch relation in nanostructured aluminum alloys by ultra-severe plastic deformation. Journal of Materials Science and Technology, 2021, 91, 78-89.	5.6	51
76	Long-time stability of metals after severe plastic deformation: Softening and hardening by self-annealing versus thermal stability. Materials Science & Engineering A: Structural Materials: Properties, Microstructure and Processing, 2018, 729, 340-348.	2.6	48
77	Impact of severe plastic deformation on microstructure and hydrogen storage of titanium-iron-manganese intermetallics. Scripta Materialia, 2016, 124, 108-111.	2.6	47
78	Optical Properties of Nanocrystalline Monoclinic Y ₂ O ₃ Stabilized by Grain Size and Plastic Strain Effects via High-Pressure Torsion. Inorganic Chemistry, 2017, 56, 2576-2580.	1.9	47
79	Hydrogen storage properties of new A3B2-type TiZrNbCrFe high-entropy alloy. International Journal of Hydrogen Energy, 2021, , .	3.8	46
80	Strengthening of A2024 alloy by high-pressure torsion and subsequent aging. Materials Science & Engineering A: Structural Materials: Properties, Microstructure and Processing, 2017, 704, 112-118.	2.6	45
81	Continuous high-pressure torsion using wires. Journal of Materials Science, 2012, 47, 473-478.	1.7	44
82	Enhanced photocatalytic hydrogen production on GaN–ZnO oxynitride by introduction of strain-induced nitrogen vacancy complexes. Acta Materialia, 2020, 185, 149-156.	3.8	44
83	High-pressure torsion of iron with various purity levels and validation of Hall-Petch strengthening mechanism. Materials Science & Engineering A: Structural Materials: Properties, Microstructure and Processing, 2019, 743, 597-605.	2.6	43
84	Phase transformations, vacancy formation and variations of optical and photocatalytic properties in TiO2-ZnO composites by high-pressure torsion. International Journal of Plasticity, 2020, 124, 170-185.	4.1	41
85	Ultrahigh hardness in nanostructured dual-phase high-entropy alloy AlCrFeCoNiNb developed by high-pressure torsion. Journal of Alloys and Compounds, 2021, 884, 161101.	2.8	41
86	Fast hydrolysis and hydrogen generation on Al-Bi alloys and Al-Bi-C composites synthesized by high-pressure torsion. International Journal of Hydrogen Energy, 2017, 42, 29121-29130.	3.8	40
87	Dynamic recrystallization and recovery during high-pressure torsion: Experimental evidence by torque measurement using ring specimens. Materials Science & Engineering A: Structural Materials: Properties, Microstructure and Processing, 2013, 559, 506-509.	2.6	37
88	Microstructural characteristics of tungsten-base nanocomposites produced from micropowders by high-pressure torsion. Acta Materialia, 2012, 60, 3885-3893.	3.8	36
89	Influence of SiC and FeSi addition on the characteristics of gray cast iron melts poured at different temperatures. Journal of Materials Processing Technology, 2005, 160, 183-187.	3.1	35
90	Improved Photocatalytic Hydrogen Evolution on Tantalate Perovskites CsTaO ₃ and LiTaO ₃ by Strain-Induced Vacancies. ACS Applied Energy Materials, 2020, 3, 1710-1718.	2.5	35

#	Article	IF	CITATIONS
91	Microstructure and microhardness of dual-phase high-entropy alloy by high-pressure torsion: Twins and stacking faults in FCC and dislocations in BCC. Journal of Alloys and Compounds, 2022, 894, 162413.	2.8	35
92	Nanocrystalline steel obtained by mechanical alloying of iron and graphite subsequently compacted by high-pressure torsion. Acta Materialia, 2015, 97, 207-215.	3.8	34
93	Real Hydrostatic Pressure in High-Pressure Torsion Measured by Bismuth Phase Transformations and FEM Simulations. Materials Transactions, 2016, 57, 533-538.	0.4	34
94	High strength and superconductivity in nanostructured niobium–titanium alloy by high-pressure torsion and annealing: Significance of elemental decomposition and supersaturation. Acta Materialia, 2014, 80, 149-158.	3.8	33
95	Fabrication of nanograined silicon by high-pressure torsion. Journal of Materials Science, 2014, 49, 6565-6569.	1.7	32
96	Superior hydrogenation properties in a Mg65Ce10Ni20Cu5 nanoglass processed by melt-spinning followed by high-pressure torsion. Scripta Materialia, 2018, 152, 137-140.	2.6	32
97	Aging Behavior of Al 6061 Alloy Processed by High-Pressure Torsion and Subsequent Aging. Metallurgical and Materials Transactions A: Physical Metallurgy and Materials Science, 2015, 46, 2664-2673.	1.1	31
98	Bulk nanocrystalline gamma magnesium hydride with low dehydrogenation temperature stabilized by plastic straining via high-pressure torsion. Scripta Materialia, 2018, 157, 54-57.	2.6	31
99	Enhanced CO2 conversion on highly-strained and oxygen-deficient BiVO4 photocatalyst. Chemical Engineering Journal, 2022, 442, 136209.	6.6	31
100	High Strength and High Uniform Ductility in a Severely Deformed Iron Alloy by Lattice Softening and Multimodal-structure Formation. Materials Research Letters, 2015, 3, 197-202.	4.1	30
101	Effect of gradient-structure versus uniform nanostructure on hydrogen storage of Ti-V-Cr alloys: Investigation using ultrasonic SMAT and HPT processes. Journal of Alloys and Compounds, 2018, 737, 337-346.	2.8	30
102	High-entropy hydrides for fast and reversible hydrogen storage at room temperature: Binding-energy engineering via first-principles calculations and experiments. Acta Materialia, 2022, 236, 118117.	3.8	30
103	Impact of TiO ₂ -II phase stabilized in anatase matrix by high-pressure torsion on electrocatalytic hydrogen production. Materials Research Letters, 2019, 7, 334-339.	4.1	29
104	Phase transformation and microstructure evolution in ultrahard carbon-doped AlTiFeCoNi high-entropy alloy by high-pressure torsion. Materials Letters, 2021, 302, 130368.	1.3	28
105	High-pressure TiO2-II polymorph as an active photocatalyst for CO2 to CO conversion. Applied Catalysis B: Environmental, 2021, 298, 120566.	10.8	28
106	Microstructural details of hydrogen diffusion and storage in Ti–V–Cr alloys activated through surface and bulk severe plastic deformation. International Journal of Hydrogen Energy, 2020, 45, 5326-5336.	3.8	27
107	Synthesis of biocompatible high-entropy alloy TiNbZrTaHf by high-pressure torsion. Materials Science & Engineering A: Structural Materials: Properties, Microstructure and Processing, 2021, 825, 141869.	2.6	27
108	Graphite to diamond-like carbon phase transformation by high-pressure torsion. Applied Physics Letters, 2013, 103, .	1.5	26

#	Article	IF	CITATIONS
109	Severe Plastic Deformation for Nanostructure Controls. Materials Transactions, 2020, 61, 2241-2247.	0.4	26
110	Gradient-structured high-entropy alloy with improved combination of strength and hydrogen embrittlement resistance. Corrosion Science, 2022, 200, 110253.	3.0	26
111	Phase Transformations in MgH ₂ –TiH ₂ Hydrogen Storage System by Highâ€Pressure Torsion Process. Advanced Engineering Materials, 2020, 22, 1900027.	1.6	25
112	Development of ultrahigh strength and high ductility in nanostructured iron alloys with lattice softening and nanotwins. Scripta Materialia, 2012, 67, 511-514.	2.6	24
113	Solid-state reactions and hydrogen storage in magnesium mixed with various elements by high-pressure torsion: experiments and first-principles calculations. RSC Advances, 2016, 6, 11665-11674.	1.7	24
114	High-resolution transmission electron microscopy analysis of nanograined germanium produced by high-pressure torsion. Materials Characterization, 2017, 132, 132-138.	1.9	23
115	Low-temperature anatase-to-rutile phase transformation and unusual grain coarsening in titanium oxide nanopowders by high-pressure torsion straining. Scripta Materialia, 2019, 162, 341-344.	2.6	23
116	Cathodic corrosion activated Fe-based nanoglass as a highly active and stable oxygen evolution catalyst for water splitting. Journal of Materials Chemistry A, 2021, 9, 12152-12160.	5.2	23
117	Unusual hardening in Ti/Al2O3 nanocomposites produced by high-pressure torsion followed by annealing. Materials Science & Engineering A: Structural Materials: Properties, Microstructure and Processing, 2011, 529, 435-441.	2.6	22
118	Novel black bismuth oxide (Bi2O3) with enhanced photocurrent generation, produced by high-pressure torsion straining. Scripta Materialia, 2020, 187, 366-370.	2.6	22
119	High-Pressure Torsion for Synthesis of High-Entropy Alloys. Metals, 2021, 11, 1263.	1.0	22
120	High-entropy alloys as anode materials of nickel - metal hydride batteries. Scripta Materialia, 2022, 209, 114387.	2.6	22
121	Phase transformation of germanium by processing through high-pressure torsion: strain and temperature effects. Philosophical Magazine Letters, 2017, 97, 27-34.	0.5	21
122	New Mg–V–Cr BCC Alloys Synthesized by High-Pressure Torsion and Ball Milling. Materials Transactions, 2018, 59, 741-746.	0.4	21
123	Evolution of lattice defects, disordered/ordered phase transformations and mechanical properties in Ni–Al–Ti intermetallics by high-pressure torsion. Journal of Alloys and Compounds, 2013, 563, 221-228.	2.8	20
124	High-pressure torsion of palladium: Hydrogen-induced softening and plasticity in ultrafine grains and hydrogen-induced hardening and embrittlement in coarse grains. Materials Science & Engineering A: Structural Materials: Properties, Microstructure and Processing, 2014, 618, 1-8.	2.6	20
125	Novel Fe-based nanoglass as efficient noble-metal-free electrocatalyst for alkaline hydrogen evolution reaction. Scripta Materialia, 2020, 188, 135-139.	2.6	20
126	Understanding the role of Ca segregation on thermal stability, electrical resistivity and mechanical strength of nanostructured aluminum. Materials Science & Engineering A: Structural Materials: Properties, Microstructure and Processing, 2020, 798, 140108.	2.6	20

#	Article	IF	CITATIONS
127	High-resolution transmission electron microscopy analysis of bulk nanograined silicon processed by high-pressure torsion. Materials Characterization, 2017, 129, 163-168.	1.9	19
128	Grain growth in nanograined aluminum oxide by high-pressure torsion: Phase transformation and plastic strain effects. Scripta Materialia, 2018, 152, 11-14.	2.6	19
129	Hydrolytic Hydrogen Production on Al–Sn–Zn Alloys Processed by High-Pressure Torsion. Materials, 2018, 11, 1209.	1.3	19
130	Photocatalytic activity of aluminum oxide by oxygen vacancy generation using high-pressure torsion straining. Scripta Materialia, 2019, 173, 120-124.	2.6	19
131	Microstructure and phase transformations of silica glass and vanadium oxide by severe plastic deformation via high-pressure torsion straining. Journal of Alloys and Compounds, 2019, 779, 394-398.	2.8	18
132	Synthesis of nanostructured biomaterials by high-pressure torsion: Effect of niobium content on microstructure and mechanical properties of Ti-Nb alloys. Materials Science & Engineering A: Structural Materials: Properties, Microstructure and Processing, 2020, 795, 139972.	2.6	18
133	Application of High-Pressure Torsion to WC–Co Ceramic-Based Composites for Improvement of Consolidation, Microstructure and Hardness. Materials Transactions, 2013, 54, 1540-1548.	0.4	17
134	Effect of temperature on solid-state formation of bulk nanograined intermetallic Al ₃ Ni during high-pressure torsion. Philosophical Magazine, 2014, 94, 876-887.	0.7	17
135	Hydrostatic Compression Effects on Fifth-Group Element Superconductors V, Nb, and Ta Subjected to High-Pressure Torsion. Materials Transactions, 2019, 60, 1472-1483.	0.4	17
136	Microstructure and defect effects on strength and hydrogen embrittlement of high-entropy alloy CrMnFeCoNi processed by high-pressure torsion. Materials Science & Engineering A: Structural Materials: Properties, Microstructure and Processing, 2022, 844, 143179.	2.6	16
137	Significant CO2 photoreduction on a high-entropy oxynitride. Chemical Engineering Journal, 2022, 449, 137800.	6.6	16
138	Production of nanograined intermetallics using high-pressure torsion. Materials Research, 2013, 16, 672-678.	0.6	15
139	Visible-Light Photocurrent in Nanostructured High-Pressure TiO ₂ -II (Columbite) Phase. Journal of Physical Chemistry C, 2020, 124, 13930-13935.	1.5	15
140	Historical Studies by Polish Scientist on Ultrafine-Grained Materials by Severe Plastic Deformation. Materials Transactions, 2019, 60, 1553-1560.	0.4	14
141	Severe plastic deformed Pd-based metallic glass for superior hydrogen evolution in both acidic and alkaline media. Scripta Materialia, 2021, 204, 114145.	2.6	14
142	Synthesis of Nanostructured TiFe Hydrogen Storage Material by Mechanical Alloying via Highâ€Pressure Torsion. Advanced Engineering Materials, 2020, 22, 2000011.	1.6	13
143	Effect of creep parameters on the steady-state flow stress of pure metals processed by high-pressure torsion. Materials Science & Engineering A: Structural Materials: Properties, Microstructure and Processing, 2022, 835, 142666.	2.6	13
144	Use of Ring Sample for High-Pressure Torsion and Microstructural Evolution with Equivalent Strain. Materials Science Forum, 0, 584-586, 191-196.	0.3	12

#	Article	IF	CITATIONS
145	Electrical resistivity mapping of titanium and zirconium discs processed by high-pressure torsion for homogeneity and phase transformation evaluation. Journal of Materials Science, 2017, 52, 6778-6788.	1.7	12
146	Critical Temperature in Bulk Ultrafine-Grained Superconductors of Nb, V, and Ta Processed by High-Pressure Torsion. Materials Transactions, 2019, 60, 1367-1376.	0.4	12
147	High-pressure torsion to induce oxygen vacancies in nanocrystals of magnesium oxide: Enhanced light absorbance, photocatalysis and significance in geology. Materialia, 2020, 11, 100670.	1.3	12
148	Highâ€pressure torsion of SiO ₂ quartz sand: Phase transformation, optical properties, and significance in geology. Journal of the American Ceramic Society, 2020, 103, 6594-6602.	1.9	11
149	FCC phase formation in immiscible Mg–Hf (magnesium–hafnium) system by high-pressure torsion. AlP Advances, 2020, 10, .	0.6	11
150	Effect of high-pressure torsion on the hydrogen evolution performances of a melt-spun amorphous Fe73.5Si13.5B9Cu1Nb3 alloy. International Journal of Hydrogen Energy, 2021, 46, 25029-25038.	3.8	11
151	Corrosion Behavior of Ultrafine-Grained CoCrFeMnNi High-Entropy Alloys Fabricated by High-Pressure Torsion. Materials, 2022, 15, 1007.	1.3	11
152	Defect detection in thin plates by ultrasonic lamb wave techniques. International Journal of Materials and Product Technology, 2006, 27, 156.	0.1	10
153	Grain refinement and superplasticity of Inconel 718 processed by Multi-Pass High-Pressure sliding. Materials Letters, 2021, 300, 130144.	1.3	10
154	Hydrostatic pressure effects on superconducting transition of nanostructured niobium highly strained by high-pressure torsion. Journal of Applied Physics, 2019, 125, .	1.1	8
155	Phase transformations in Al-Ti-Mg powders consolidated by high-pressure torsion: Experiments and first-principles calculations. Journal of Alloys and Compounds, 2021, 889, 161815.	2.8	8
156	Influence of nanotwins on hydrogen embrittlement of TWIP (twinning-induced plasticity) steel processed by high-pressure torsion. Materials Science & Engineering A: Structural Materials: Properties, Microstructure and Processing, 2020, 783, 139273.	2.6	7
157	Flaw detection improvement of digitised radiographs by morphological transformations. Insight: Non-Destructive Testing and Condition Monitoring, 2005, 47, 625-630.	0.3	6
158	Parameters Influencing Steady-State Grain Size of Pure Metals Processed by High-Pressure Torsion. Materials Science Forum, 0, 706-709, 3034-3039.	0.3	6
159	Magnetic measurements of hydrogen desorption from palladium hydride PdH0.64 prepared by severe plastic deformation. Journal of Applied Physics, 2020, 127, .	1.1	6
160	In-service corrosion evaluation in pipelines using gamma radiography – a numerical approach. Insight: Non-Destructive Testing and Condition Monitoring, 2004, 46, 396-398.	0.3	5
161	Correlation of Physical Parameters with Steady-State Hardness of Pure Metals Processed by High-Pressure Torsion. Materials Science Forum, 2010, 667-669, 683-688.	0.3	5
162	Contactless measurement of electrical conductivity for bulk nanostructured silver prepared by high-pressure torsion: A study of the dissipation process of giant strain. Journal of Applied Physics, 2017, 122, .	1.1	5

#	Article	IF	CITATIONS
163	High Pressure Torsion of Pure Ti: Effect of Pressure and Strain on Allotropy. Advanced Materials Research, 0, 89-91, 171-176.	0.3	4
164	Superplasticity of nanostructured Ti-6Al-7Nb alloy with equiaxed and lamellar initial microstructures processed by High-Pressure Torsion. IOP Conference Series: Materials Science and Engineering, 2017, 194, 012041.	0.3	4
165	A radiographic calibration method for eddy current testing of heat exchanger tubes. Insight: Non-Destructive Testing and Condition Monitoring, 2004, 46, 594-597.	0.3	4
166	Effect of Homogenization on Microstructure and Hardness of Arc-Melted FeCoNiMn High Entropy Alloy During High-Pressure Torsion (HPT). Journal of Materials Engineering and Performance, 2022, 31, 5080-5089.	1.2	4
167	Influence of inoculant and/or SiC addition on characteristics of grey cast iron. International Journal of Cast Metals Research, 2004, 17, 147-151.	0.5	3
168	Scattering and image contrast simulation for double wall radiography of pipes. International Journal of Pressure Vessels and Piping, 2007, 84, 441-450.	1.2	3
169	Phase transformations during high-pressure torsion (HPT) in titanium, cobalt and graphite. IOP Conference Series: Materials Science and Engineering, 2014, 63, 012099.	0.3	3
170	Glycine amino acid transformation under impacts by small solar system bodies, simulated via high-pressure torsion method. Scientific Reports, 2022, 12, 5677.	1.6	3
171	Three-dimensional mapping of non-complex specimens by image processing and optical density evaluation of digitised radiographs. Insight: Non-Destructive Testing and Condition Monitoring, 2009, 51, 315-320.	0.3	2
172	High Strength and High Ductility in Nanostructured Aluminium-Based Intermetallics Produced by High-Pressure Torsion. Materials Science Forum, 2013, 765, 558-562.	0.3	2
173	Microstructure Formation of High Pressure Torsion Processed (α + γ) Two Phase Stainless Steel. Materials Science Forum, 2016, 879, 1365-1368.	0.3	2
174	High Strength and Ductility in Ball-Milled Titanium Powders Consolidated by High-Pressure Torsion. Materials Science Forum, 0, 654-656, 1239-1242.	0.3	1
175	Formation of Bulk Nanostructured Al ₃ Ni from Elemental Micropowders Using High-Pressure Torsion. Materials Science Forum, 0, 765, 378-382.	0.3	1
176	Influence of high-pressure torsion on formation/destruction of nano-sized spinodal structures. AIP Conference Proceedings, 2018, , .	0.3	1
177	Influence of Cu doping and high-pressure torsion on electrochemical performance of lithium-rich cathode material. Journal of Physics: Conference Series, 2021, 1750, 012077.	0.3	1
178	High Resolution TEM Observation of Nanocrystalline Silicon Fabricated by High Pressure Torsion (HPT). Microscopy and Microanalysis, 2015, 21, 1783-1784.	0.2	0
179	GRAIN REFINEMENT AND MICROSTRUCTURE EVOLUTION IN ALUMINUM A2618 ALLOY BY HIGH-PRESSURE TORSION. Jurnal Teknologi (Sciences and Engineering), 2016, 78, .	0.3	0
180	Significance of High-Pressure Torsion (HPT) on Solid-State Hydrogen Storage Properties. , 2017, , .		0

Significance of High-Pressure Torsion (HPT) on Solid-State Hydrogen Storage Properties. , 2017, , . 180